

Supporting information

Polar NiFe Layered Double Hydroxides Nanosheets for Enhancing the Performance of Lithium-Sulfur Batteries

Lujing Liu^{a,c#}, Kai Meng^{a,b#}, Zhijun Jia^{a,*}, Yi Wang^{a,*}, Tao Qi^{a,*}

^aNational Engineering Laboratory for Hydrometallurgical Cleaner Production Technology,

Institute of Process Engineering, Chinese Academy of Sciences, Beijing 100190, China

^bUniversity of Chinese Academy of Sciences, Beijing 100049, China

^cNational Science Library, Chinese Academy of Sciences, Beijing 100190, China

#These authors contributed equally.

*Corresponding Authors: Y. Wang, Fax: (+86) 10 82544848-802, Tel: (+86) 10 82544967, E-mail: wangyi@ipe.ac.cn ; Z. Jia, E-mail: zjia@ipe.ac.cn ; T. Qi, E-mail: tqi@ipe.ac.cn

Supplementary figures

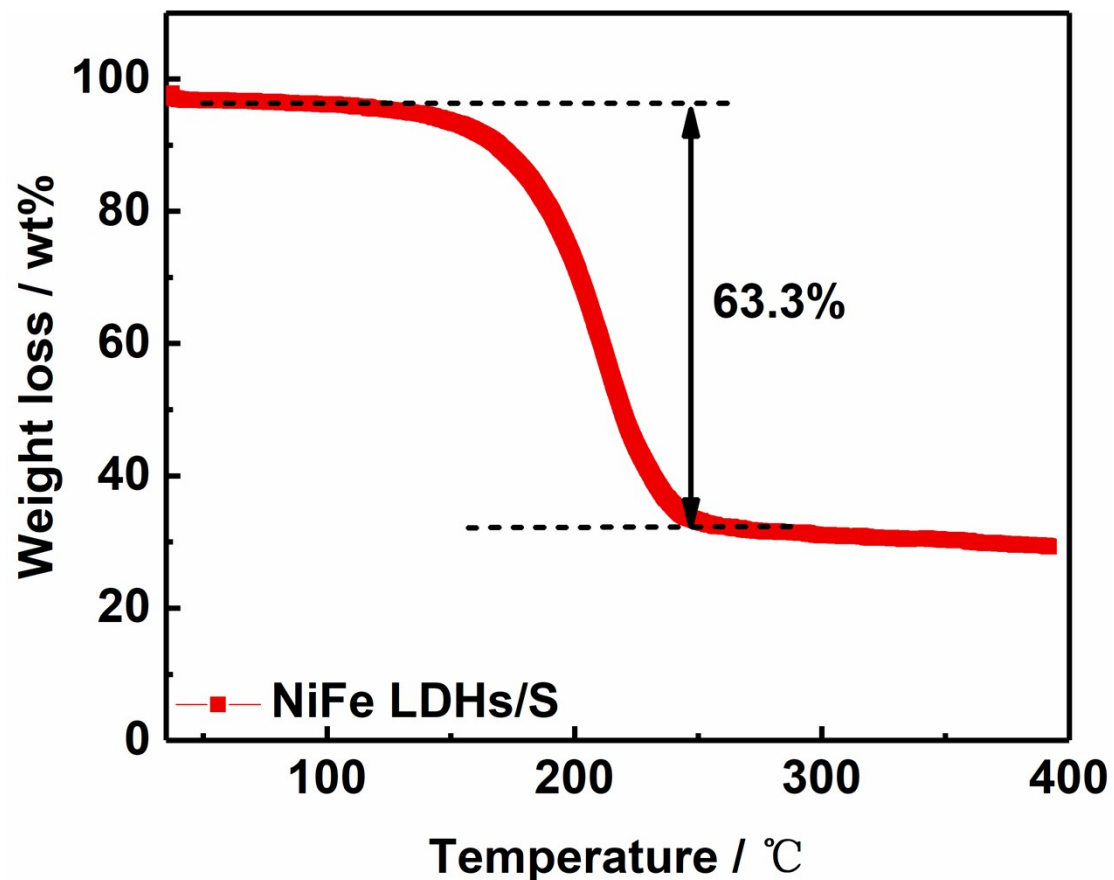


Figure S1. Thermogravimetric analysis of NiFe LDHs/S.

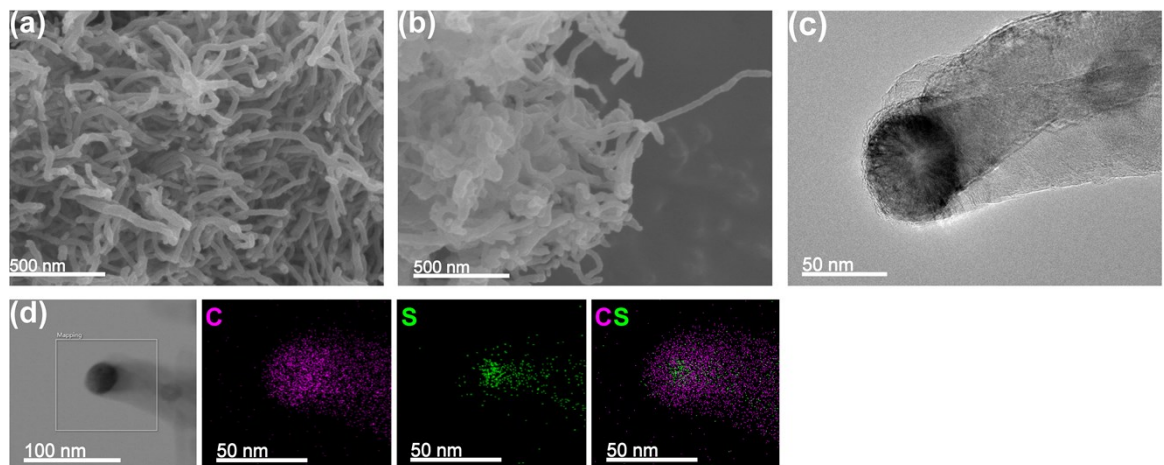


Figure S2. SEM images of (a) CNTs and (b) CNTs/S. (c) TEM image of CNTs/S and (d) corresponding EDS mapping images.

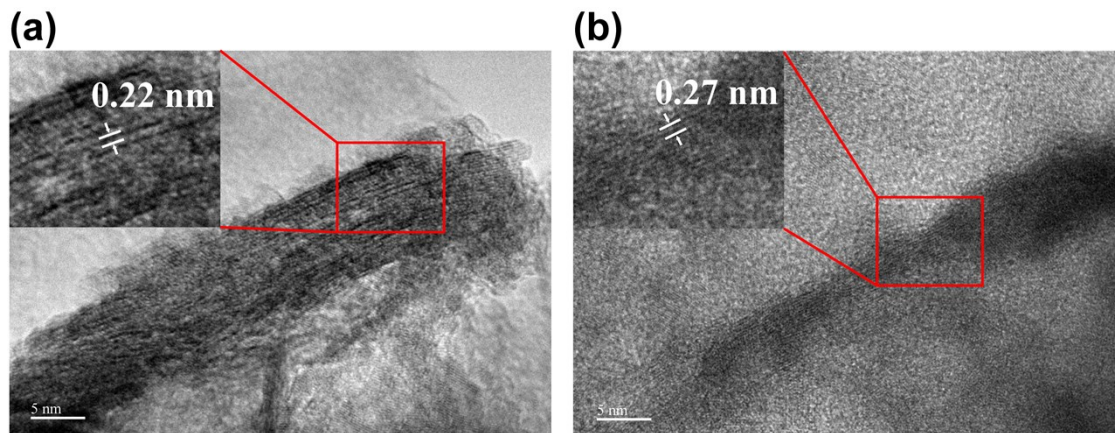


Figure S3. TEM images of (a) the layer of NiFe LDHs and (b) the layer of NiFe LDHs/S.

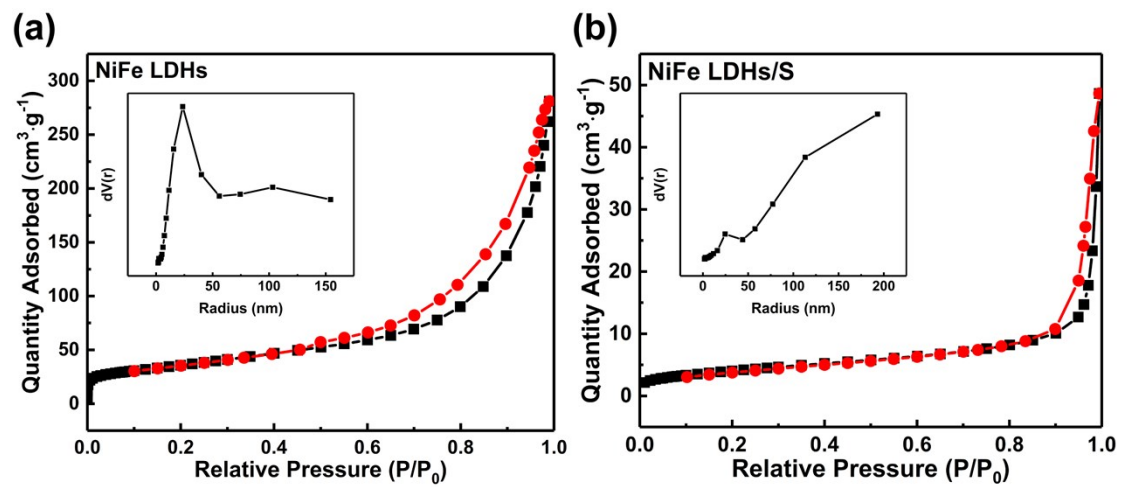


Figure S4. Nitrogen adsorption/desorption isotherms and pore size distribution (insets) of (a) NiFe LDHs and (b) NiFe LDHs/S.

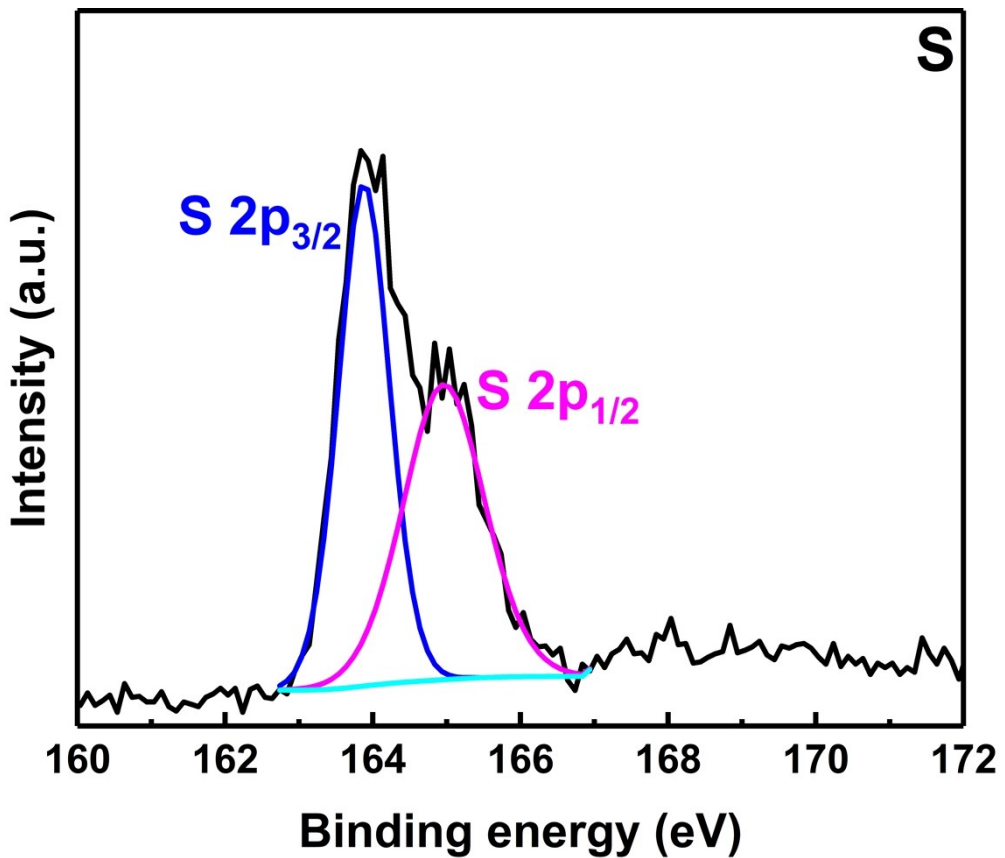


Figure S5. High-resolution XPS spectrum of S 2p for pure sulfur.

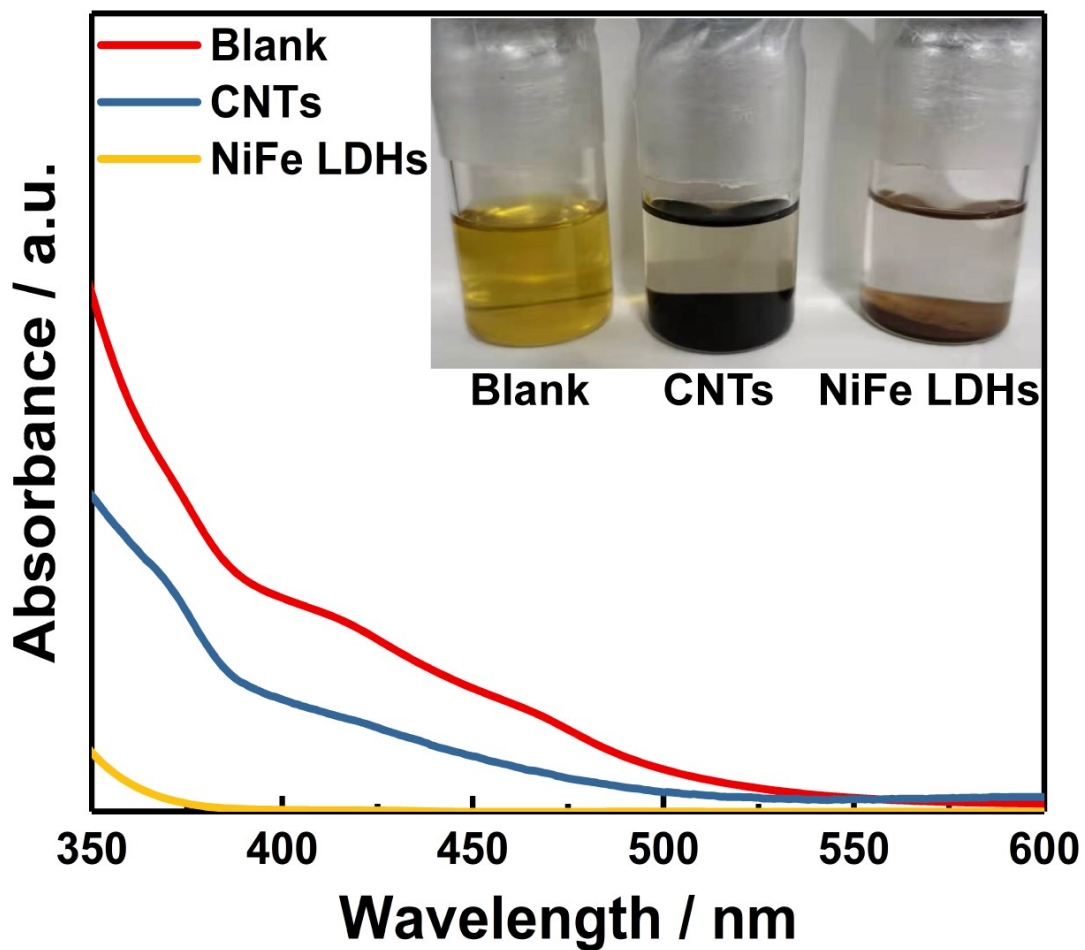


Figure S6. UV-vis absorption spectra and visual images (inset) of polysulfide solution before and after the addition of CNTs or NiFe LDHs.

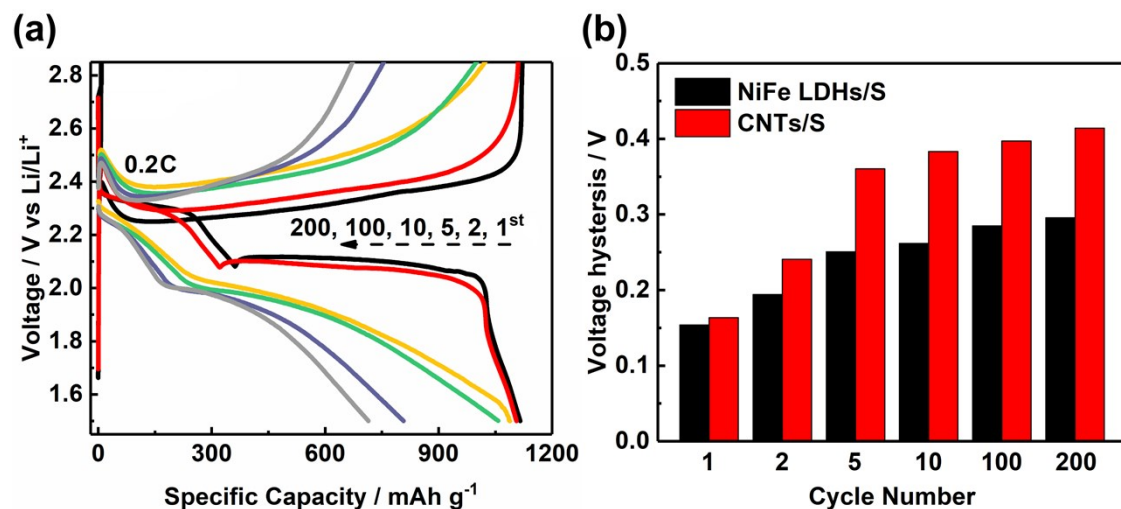


Figure S7. (a) Charge/discharge curves of CNTs/S at 0.2 C. (b) Voltage hysteresis of the NiFe LDHs/S and CNTs/S electrodes at various cycles.

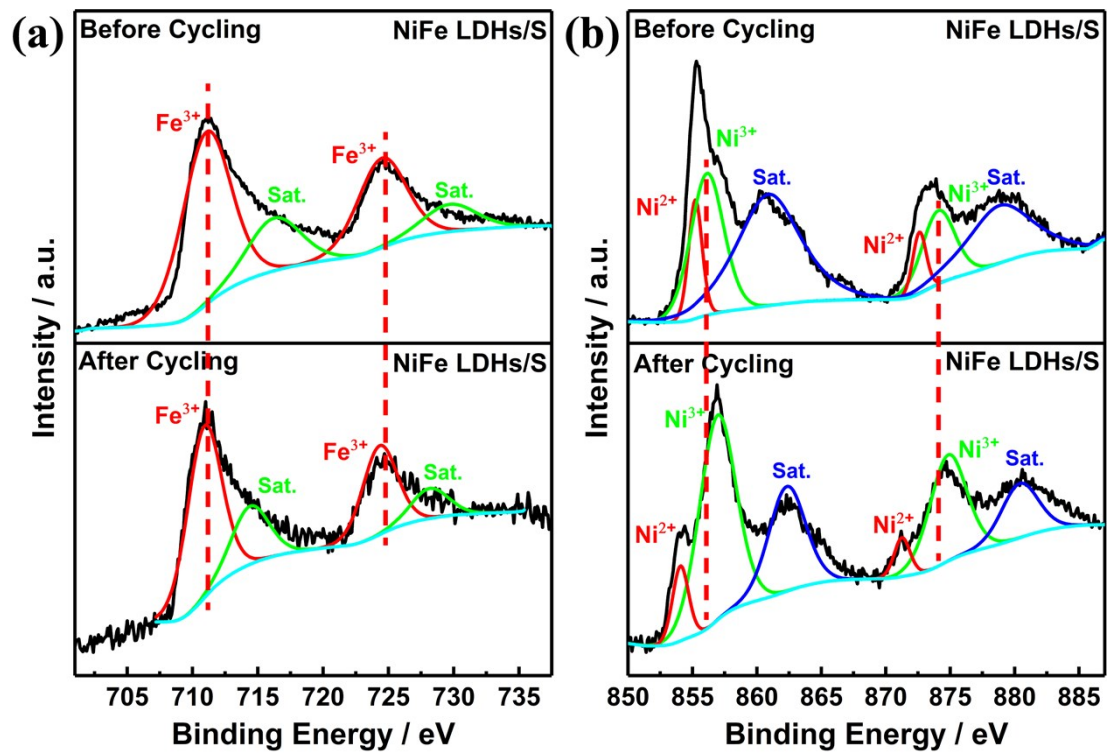


Figure S8. High-resolution XPS spectra of (a) Ni 2p and (b) Fe 2p for NiFe LDHs/S before and after 400 cycles at a rate of 0.2 C.

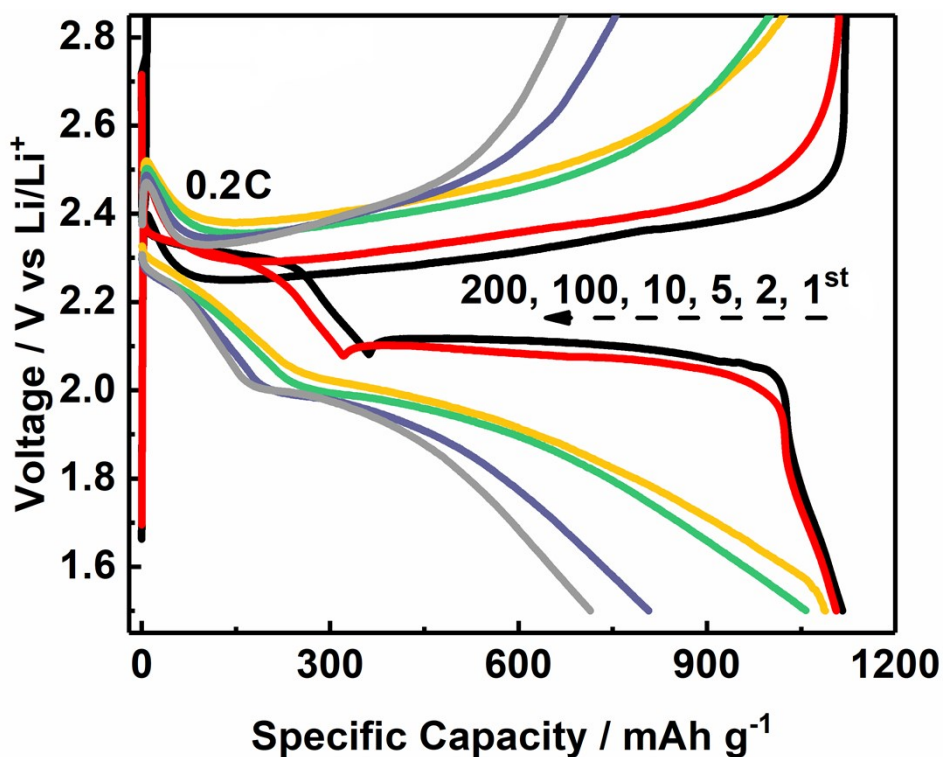


Figure S9. (a) Cycle performance comparison among NiFe LDHs/S, NiFe LDHs-20%/S and NiFe LDHs-40%/S.

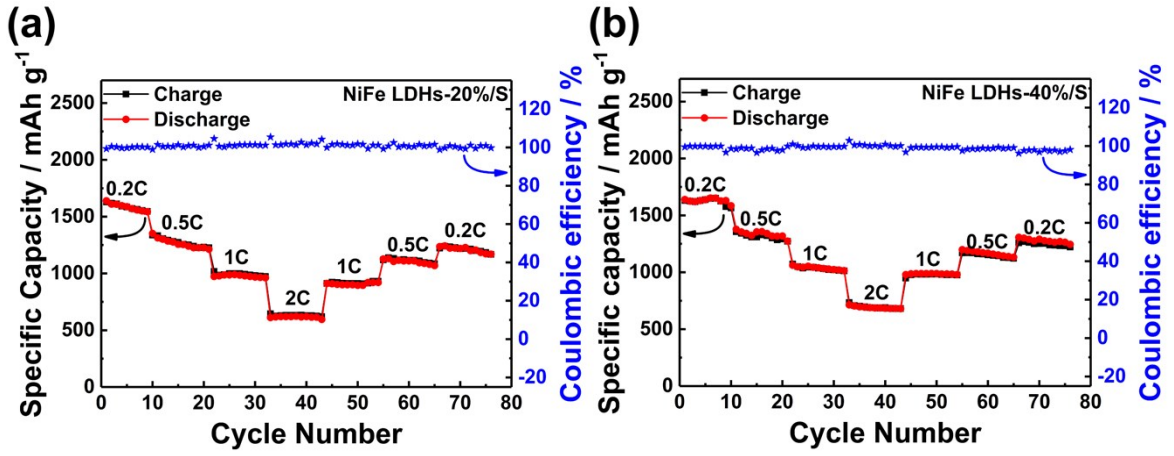


Figure S10. Rate capabilities of (a) NiFe LDHs-20%/S and (b) NiFe LDHs-40%/S at various current densities from 0.2 to 2.0 C.

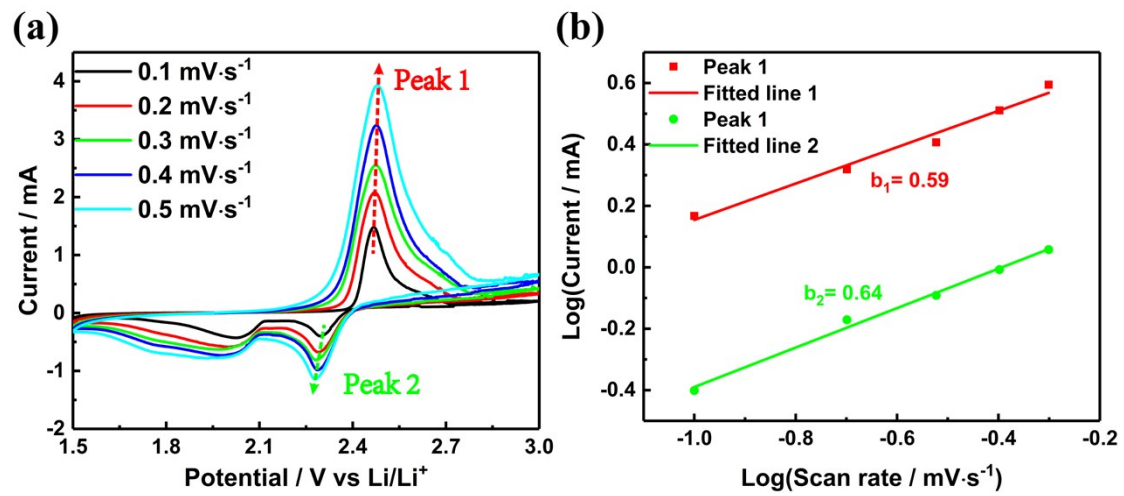


Figure S11. (a) CV curves of NiFe LDHs/S cathode at different scan rates and (b) fitted lines of log (peak current) and log (scan rate).

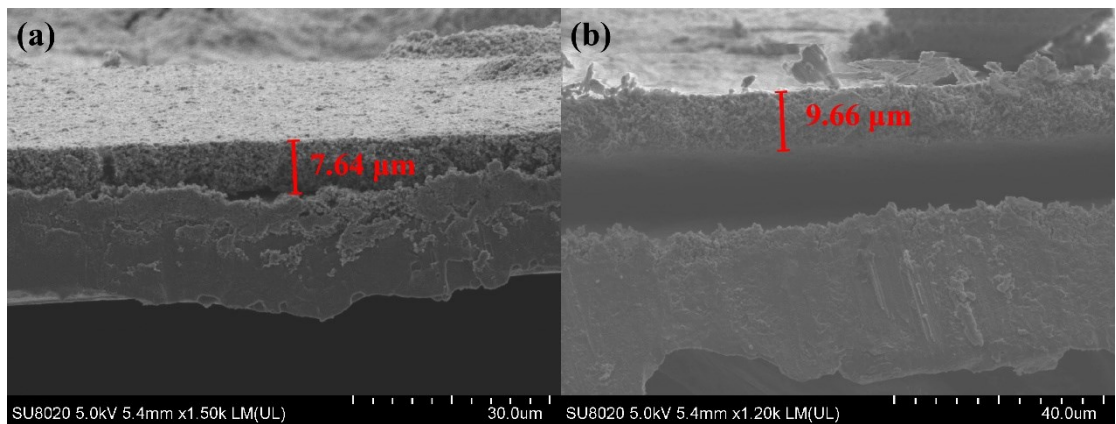


Figure S12. SEM images of typical side-views of NiFe LDHs/S cathode in Li-S cells (a) before and (b) after 1000 cycles.

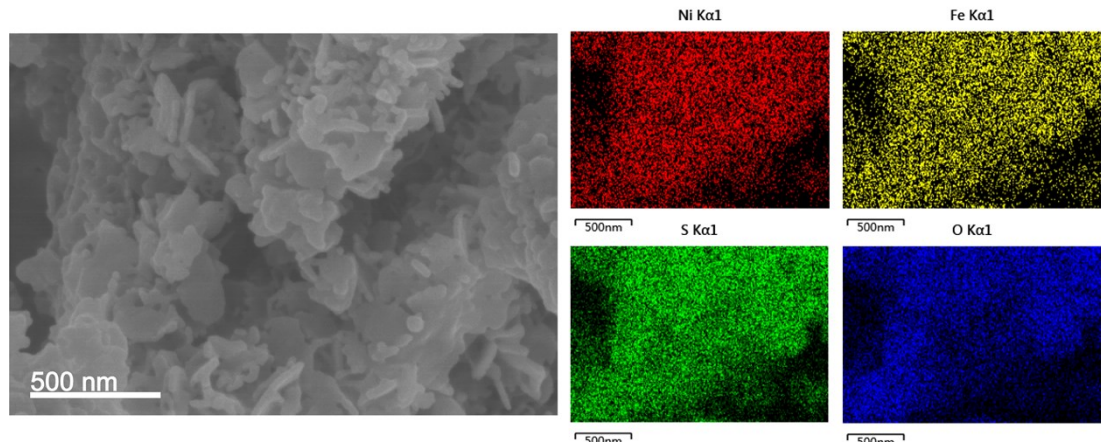


Figure S13. SEM image and EDS mapping images of NiFe LDHs/S after 1000 cycles.

Supplementary table

Table S1. Comparison of the electrochemical performance of NiFe LDHs/S at 0.2 C with that of other reported state-of-the-art cathode materials.

Cathode materials	Initial capacity (mAh g ⁻¹)	Cycles	Capacity after cycles	Capacity decay (% per cycle)	Ref.
NiFe LDHs/S	1633.5	400	1103	0.08	This work
CNTs/S	1115.8	400	640	0.11	This work
3D GF-rGO/S	1000	350	638	0.1	1
Li ₂ S@TiS ₂	806	150	693	0.09	2
MWCNT@S	1035	100	602	0.42	3
GS-MWCNT@S	1396	100	844	0.40	3
S/ZIF-8-NS-C	1226	100	800	0.34	4
VO ₂ -rGO/S	1180	200	896	0.12	5
rGO/S	985	200	493	0.25	5
S/rGO-La(OH) ₃	861	50	574	0.67	6
TMTD-S	685	200	540	0.11	7
C@NiSe ₂ /S	1250	200	1025	0.34	8
S@NiCo-DH@RC	1132.3	250	971.9	0.14	9
S@Ni/Fe LDH	1091	200	724.5	0.17	10

Table S2. Comparison of the electrochemical performance of NiFe LDHs/S at 2 C with that of other reported state-of-the-art cathode materials.

Cathode materials	Initial capacity (mAh g ⁻¹)	cycles	Capacity after cycles	Capacity decay (% per cycle)	Ref.
NiFe LDHs/S	836.1	1000	631.6	0.024	This work
MWCNT@S	1035	100	602	0.42	3
GS-MWCNT@S	1396	100	844	0.40	3
S@NiCo-DH@RC	871.5	1500	675.6	0.015	9
S@GFS-15	891.7	1000	396.8	0.037	11
C@WS ₂ /S	563	1500	502	0.00072	12
N-Co ₃ O ₄ @N-C/rGO-S	~900	1000	611	0.032	13
GA-DR-MoS ₂ /S	762	500	609.6	0.042	14
CP(S-PMAT)/C	739	1000	495	0.040	15
CC@CoP/C-S	923	600	833	0.016	16
MCM/Nb ₂ O ₅ /S	~1200	500	650	0.092	17
SiO ₂ @HC/S	776	400	603	0.056	18

Evaluation of the lithium ions diffusion coefficients

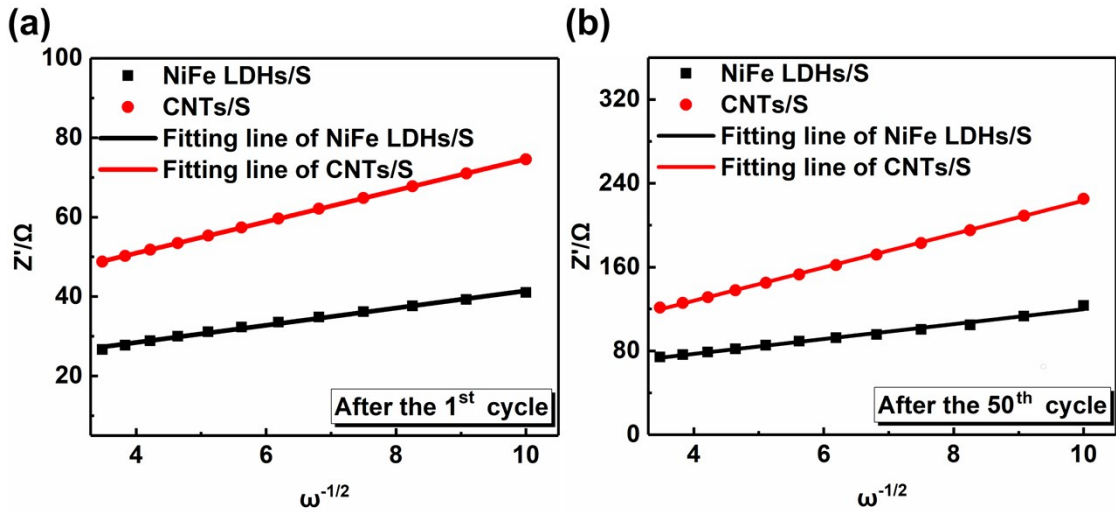


Figure S14. Variations and fittings between Z' and $\omega^{-1/2}$ in the low frequency region after (a) the 1st and (b) the 50th cycles.

In order to evaluate the lithium ions diffusion coefficients (D), the linear relations between Z' and $\omega^{-1/2}$ for NiFe LDHs/S and CNTs/S electrodes were fitted in Figure S14(a) and S14(b), respectively. The Li^+ diffusion coefficient (D) can be calculated through the following equation¹⁹:

$$[1]$$

For the calculation of D , the value of σ needs to be identified. Considering the proportional relationship between Z' and $\omega^{-1/2}$ ($Z' \propto \sigma\omega^{-1/2}$, as shown in Figure S11), the value of σ can be obtained by the linear fitting of Z' and $\omega^{-1/2}$ and the results are shown in Table I. According to the equation [1], the order of D is NiFe LDHs/S (after the 1st cycle) > CNTs/S (after the 1st cycle) > NiFe LDHs/S (after the 50th cycle) > CNTs/S (after the 50th cycle).

References

1. G. Hu, C. Xu, Z. Sun, S. Wang, H.-M. Cheng, F. Li and W. Ren, *Adv. Mater.*, 2016, **28**, 1603-1609.
2. Z. W. Seh, J. H. Yu, W. Li, P.-C. Hsu, H. Wang, Y. Sun, H. Yao, Q. Zhang and Y. Cui, *Nature Commun.*, 2014, **5**, 5017.
3. R. Chen, T. Zhao, J. Lu, F. Wu, L. Li, J. Chen, G. Tan, Y. Ye and K. Amine, *Nano Lett.*, 2013, **13**, 4642-4649.
4. Q. Wu, X. Zhou, J. Xu, F. Cao and C. Li, *J. Energy Chem.*, 2019, **38**, 94-113.
5. J. Xu, T. Li, W. Zhang, W. Wu, Y. Jin, X. Zhang, D. Su and G. Wang, *J. Alloys Compd.*, 2019, **804**, 549-553.
6. Y. Tian, Y. Zhao, Y. Zhang, L. Ricardez-Sandoval, X. Wang and J. Li, *ACS Appl. Mater. Interfaces*, 2019, **11**, 23271-23279.
7. H. Xu, Y. Shi, S. Yang and B. Li, *J. Power Sources*, 2019, **430**, 210-217.
8. M. X. Wang, L. S. Fan, X. Wu, Y. Qiu, B. Guan, Y. Wang, N. Q. Zhang and K. N. Sun, *J. Mater. Chem. A.*, 2019, **7**, 15302-15308.
9. L. Zhang, Z. X. Chen, N. C. Dongfang, M. X. Li, C. Z. Diao, Q. S. Wu, X. Chi, P. L. Jiang, Z. D. Zhao, L. Dong, R. C. Che, K. P. Loh and H. B. Lu, *Adv. Energy Mater.*, 2018, **8**, 12.
10. J. Zhang, Z. Li, Y. Chen, S. Gao and X. W. Lou, *Angew. Chem., Int. Ed.*, 2018, **57**, 10944-10948.
11. H. Zhang, Q. Gao, X. Tian, Z. Li, P. Xu and H. Xiao, *Electrochim. Acta*, 2019, **319**, 472-480.
12. T. Lei, W. Chen, J. Huang, C. Yan, H. Sun, C. Wang, W. Zhang, Y. Li and J. Xiong, *Adv. Energy Mater.*, 2017, **7**.
13. J. Xu, W. Zhang, Y. Chen, H. Fan, D. Su and G. Wang, *J. Mater. Chem. A.*, 2018, **6**, 2797-2807.
14. M. Liu, C. Zhang, J. Su, X. Chen, T. Ma, T. Huang and A. Yu, *ACS Appl. Mater. Interfaces*, 2019, **11**, 20788-20795.
15. S. Zeng, L. Li, L. Xie, D. Zhao, N. Wang and S. Chen, *ChemSusChem*, 2017, **10**, 3378-3386.
16. Z. Wang, J. Shen, J. Liu, X. Xu, Z. Liu, R. Hu, L. Yang, Y. Feng, J. Liu, Z. Shi, L. Ouyang, Y. Yu and M. Zhu, *Adv. Mater.*, 2019, **31**, 1902228.
17. Y. Tao, Y. Wei, Y. Liu, J. Wang, W. Qiao, L. Ling and D. Long, *Energy Environ. Sci.*, 2016, **9**, 3230-3239.
18. R. Wang, K. Wang, S. Gao, M. Jiang, M. Zhou, S. Cheng and K. Jiang, *Nanoscale*, 2017, **9**, 14881-14887.
19. M. He, L. Yuan, W. Zhang, X. Hu and Y. Huang, *J. Phys. Chem. C*, 2011, **31**, 15703-15709.